Supplementary Information

Tissue adhesive, antibacterial, and macrophage reprogramming hydrogel for sealing colorectal anastomotic leakage and promoting healing

Yuzhou Zhu[a], Zhongwu Bei[a] ,Tianying Luo[a], Ziqiang Wang[a], Zhiyong Qian*[a]

a. Colorectal Cancer Center, Department of General Surgery, Cancer Center and State Key Laboratory of Biotherapy, West China Hospital, Sichuan University, Chengdu, 610041, People's Republic of China.

*Correspondence: Zhiyong Qian\

E-mail: anderson-qian@163.com

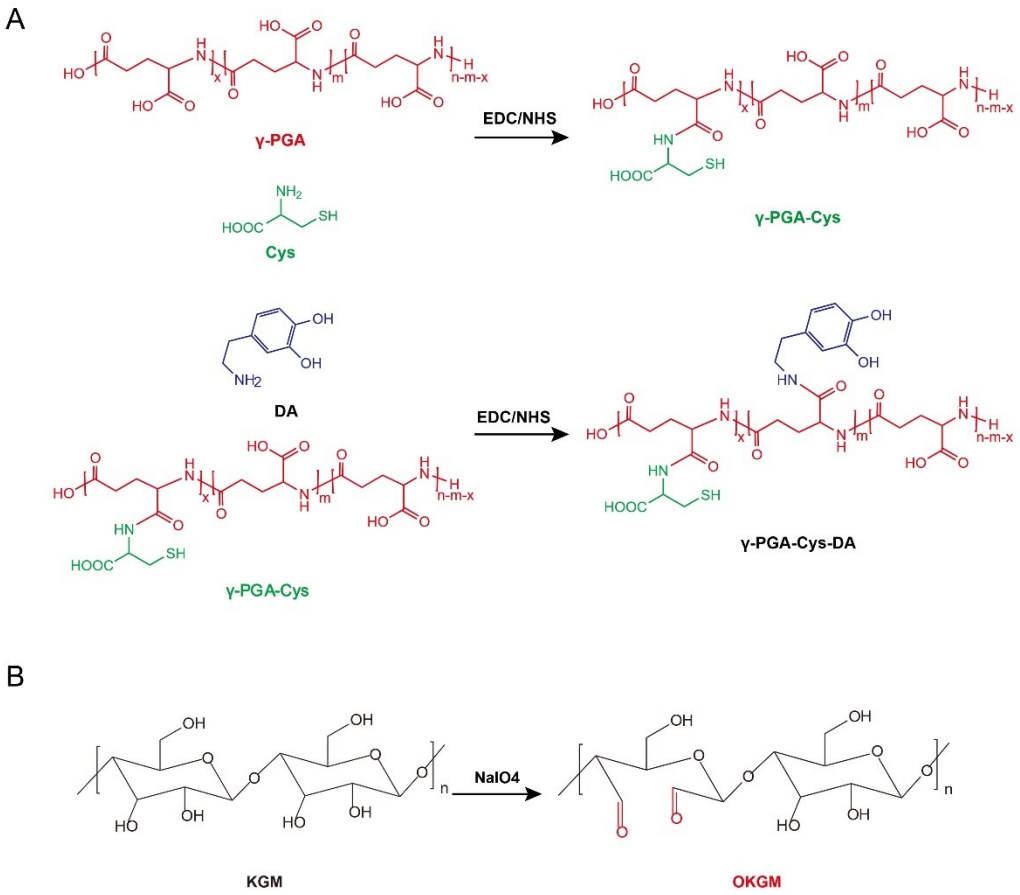

Figure S1. Synthetic routes for the two hydrogel precursors. (A) Reaction scheme for the synthesis of γ-PGA-Cys-DA. (B) Reaction scheme for the oxidation of KGM to OKGM.

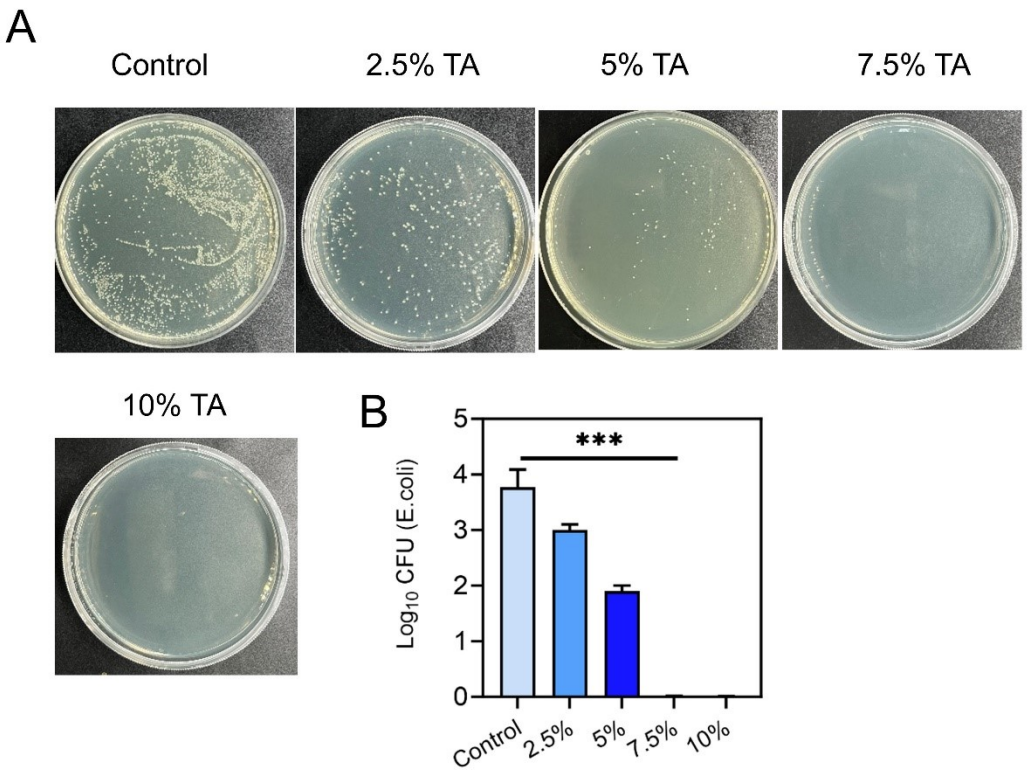

Figure S2. Influence of tannic acid (TA) content on antibacterial performance. （A） Representative images. (B) Quantification of bactericidal survival rate. Note: TA percentage refers to component B; the final hydrogel TA concentration is half of that value (due to 1:1 mixing of components A and B).

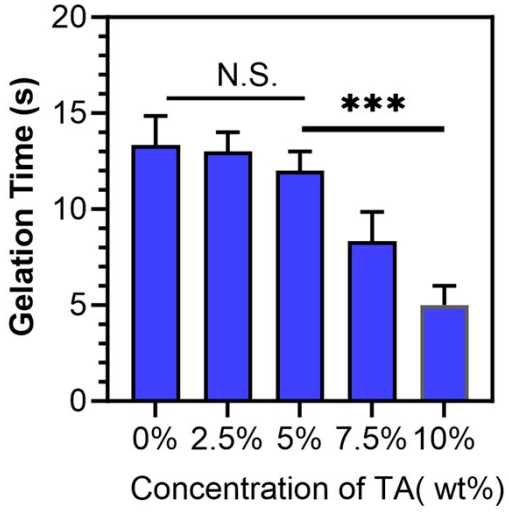

Figure S3. Effect of TA content on hydrogel gelation time (with component A fixed at 15 wt% γ-PGA-Cys-DA and component B containing 15 wt% OKGM). *Note:* TA percentages refer to component B; the actual TA content in the mixed hydrogel is half of the listed value (since components A and B are mixed 1:1). n = 3; N.S., not significant, * $p < 0.05$, ** $p < 0.01$, *** $p < 0.001$.

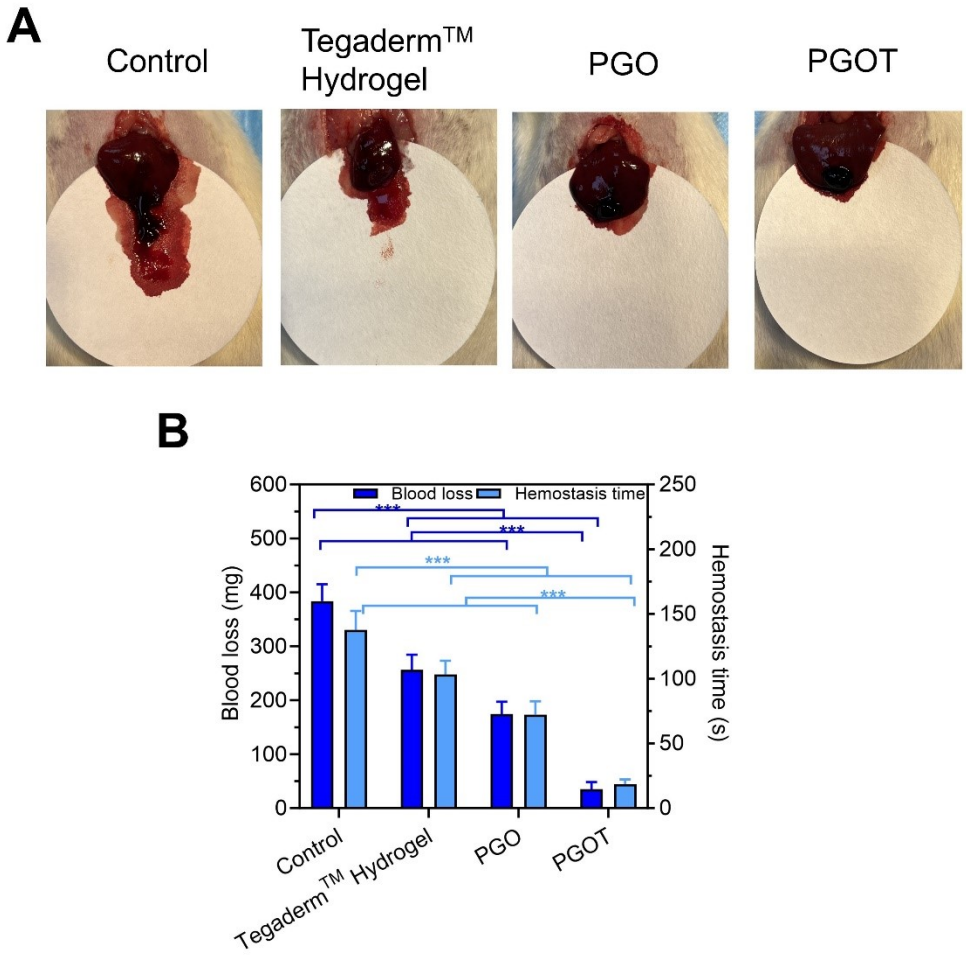

Figure S4. Hemostatic performance of hydrogels in a rat liver incision model. (A) Representative images of the liver bleeding site treated with different hydrogels. (B) Quantification of hemostatic efficacy, including blood loss volume and bleeding time for each group. n = 5; N.S., not significant, * $p < 0.05$, ** $p < 0.01$, *** $p < 0.001$.

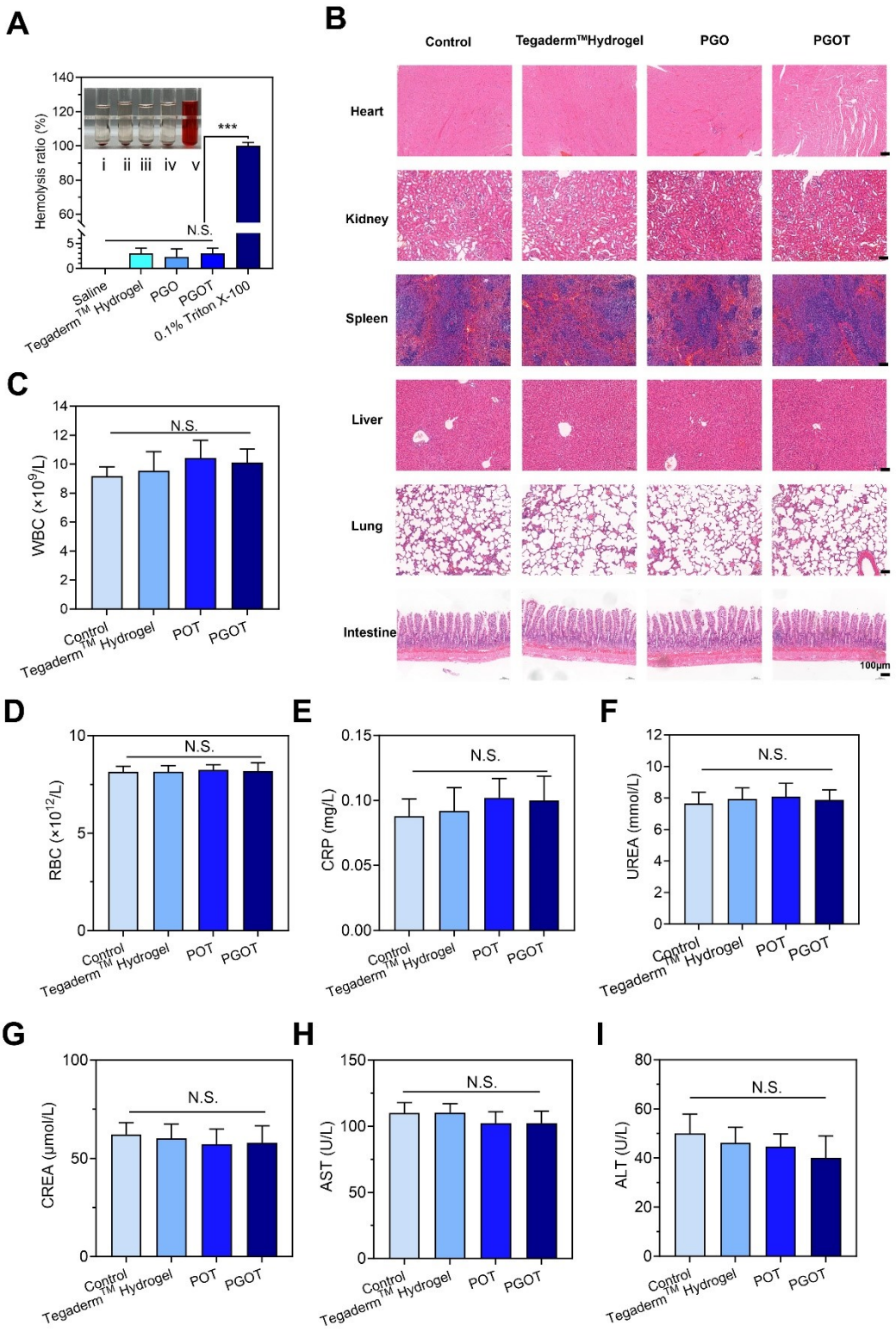

Figure S5. Biosafety evaluation of the hydrogel. (A) Hemolysis assay. (B) H&E-stained sections of major organs 21 days after hydrogel implantation. (C–I) Blood biochemistry and hematology at Day 21 after hydrogel implantation. n = 5; N.S., not significant, *

$p < 0.05$, ** $p < 0.01$, *** $p < 0.001$.

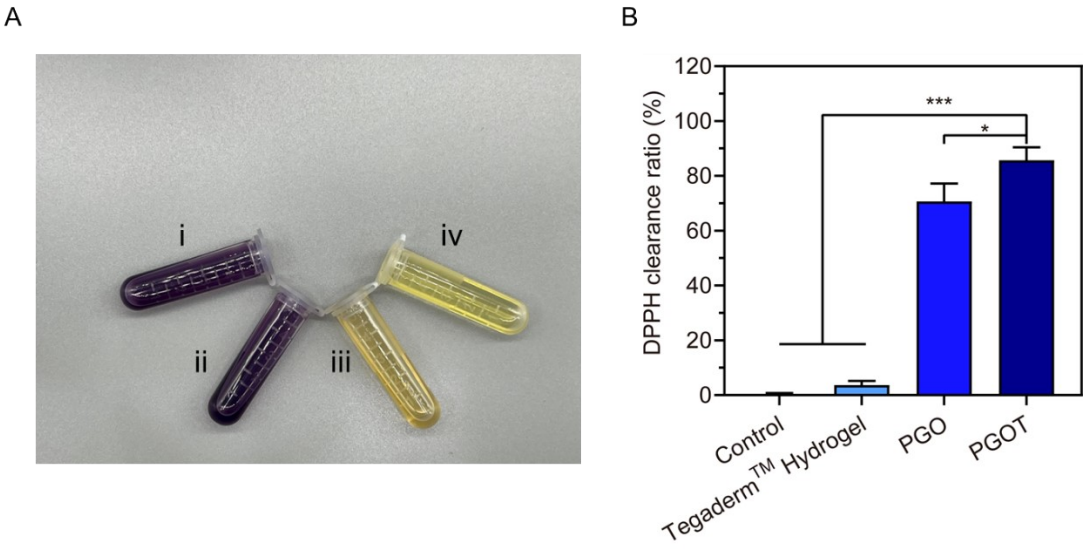

Figure S6. Antioxidant Activity of Hydrogels**.** (A) Color change of DPPH methanol solution after 30 minutes of incubation with Control (i), Tegaderm™ Hydrogel (ii), PGO (iii), and PGOT (iv). (B) DPPH scavenging efficiency of each group, indicating the antioxidant potential of the hydrogels. n = 3; N.S., not significant, * $p < 0.05$, ** $p < 0.01$, *** $p < 0.001$.

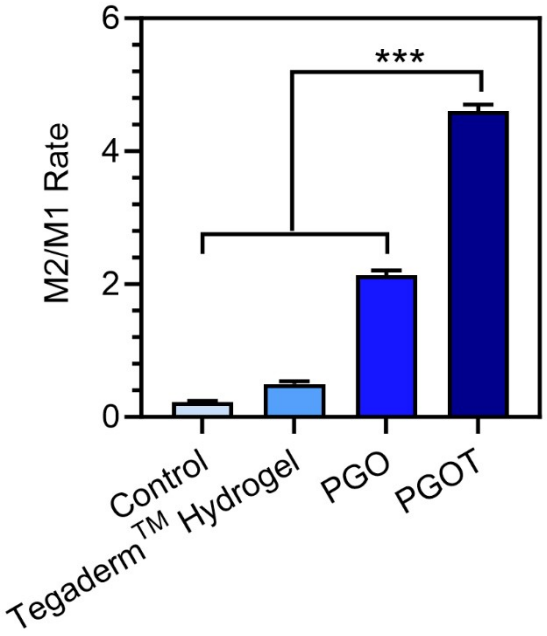

Figure S7. Corresponding M2/M1 ratio of macrophages for each group. n = 3; N.S., not significant, * $p < 0.05$, ** $p < 0.01$, *** $p < 0.001$.

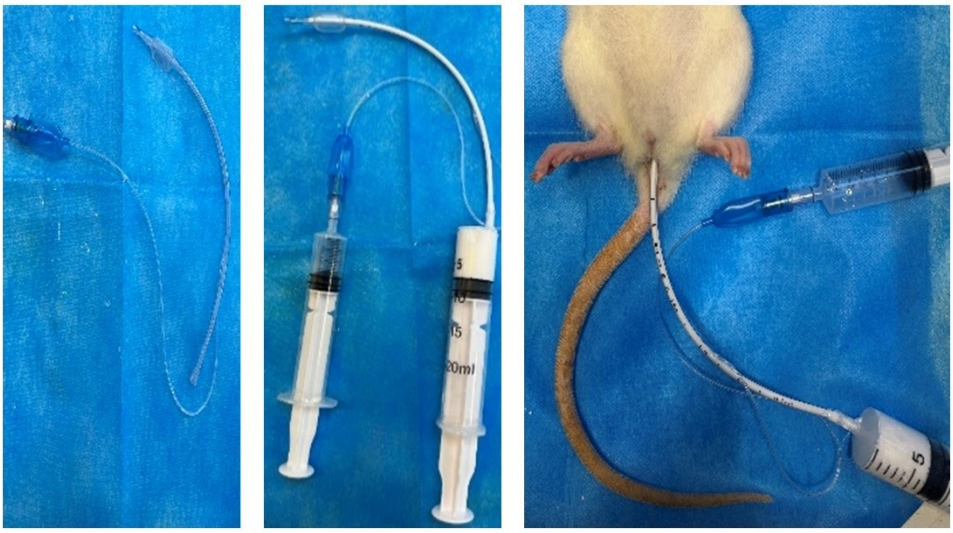

Figure S8. Illustration of the rectal contrast injection for leak detection. A catheter is inserted via the rectum into the rat's colon, and a tiny balloon on the catheter is inflated to hold it in place. Contrast agent is then injected through the catheter into the intestine

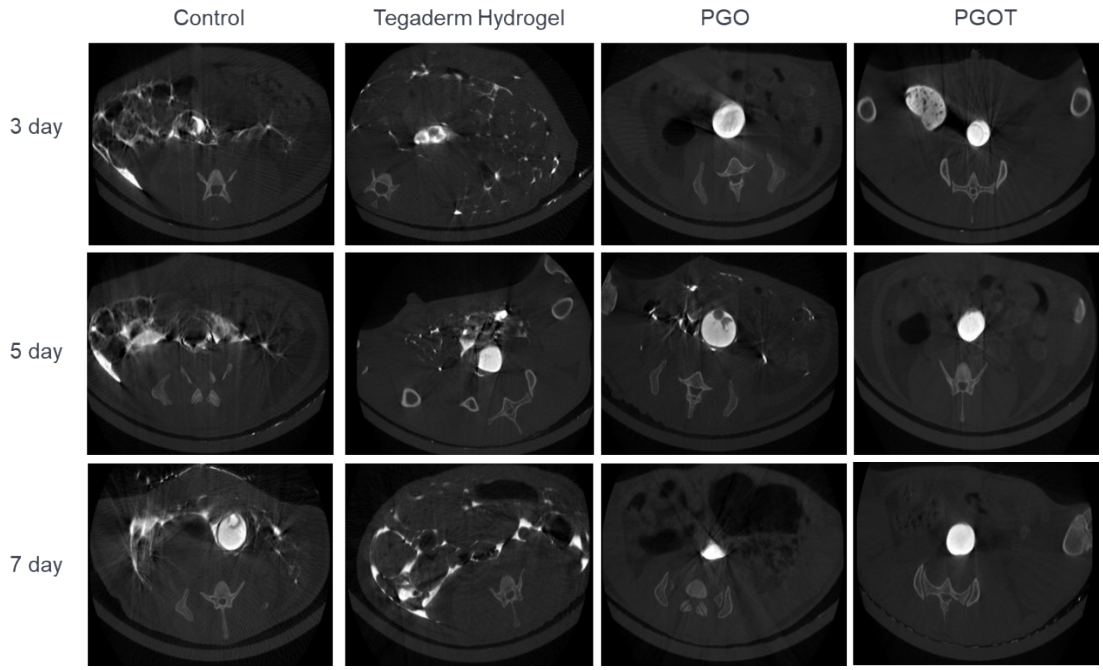

Figure S9. Representative contrast CT images of rat intestines. In rats without anastomotic leakage (PGOT group), the contrast agent (appearing white) remains confined within the intestinal lumen, whereas in rats with leakage (control and Tegaderm™ hydrogel), the agent spreads into the peritoneal cavity.

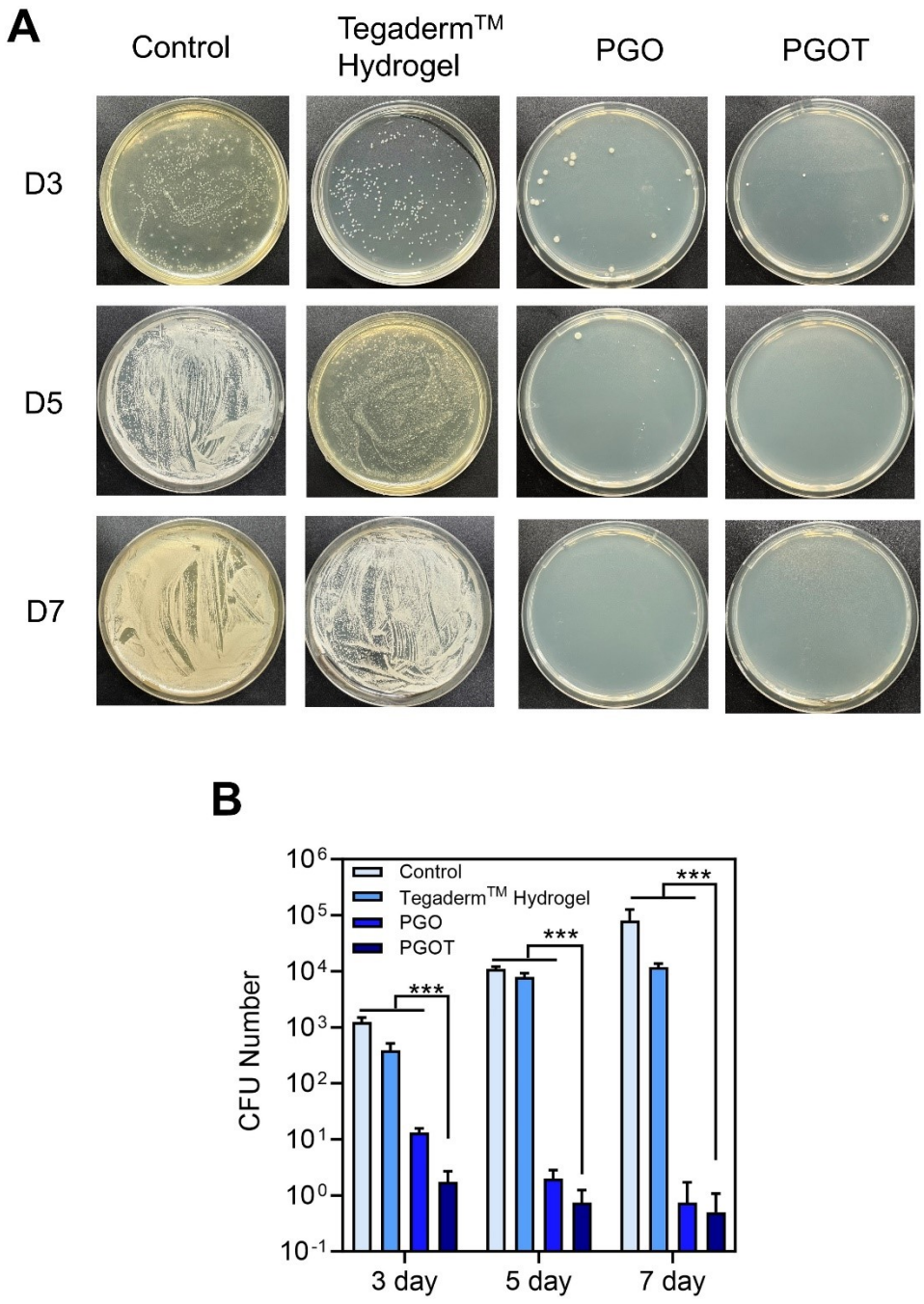

Figure S10. Postoperative intraperitoneal bacterial load in each group. (A) representative images. (B) quantification analysis. n = 5; N.S., not significant, * $p < 0.05$, ** $p < 0.01$, *** $p < 0.001$.

Table S1. Composition of PGO and PGOT hydrogels (wt%).

	γ-PGA-Cys-DA	OKGM	TA	PBS
PGO	7.5 wt%	7.5 wt%	0 wt%	85 wt%
PGOT	7.5% wt%	7.5 wt%	2.5 wt%	82.5 wt%

Note: PGO and PGOT hydrogels are formed by mixing two precursor solutions (Part A and Part B) in a 1:1 volume ratio. All component concentrations are expressed as weight percentages of the total combined system. **Abbreviations:** γ-PGA-Cys-DA = γ-poly(glutamic acid) modified with dopamine and L-cysteine; OKGM = oxidized konjac glucomannan; TA = tannic acid.